

POTENTIAL OF THE NEUTRON LLOYD'S MIRROR INTERFEROMETER FOR THE SEARCH FOR NEW INTERACTIONS

*Yu. N. Pokotilovski**

*Joint Institute for Nuclear Research
141980, Dubna, Moscow Region, Russia*

Received September 18, 2012

We discuss the potential of the neutron Lloyd's mirror interferometer in a search for new interactions at small scales. We consider three hypothetical interactions that may be tested using the interferometer. The chameleon scalar field proposed to solve the enigma of accelerating expansion of the Universe produces interaction between particles and matter. The axion-like spin-dependent coupling between a neutron and nuclei or/and electrons may result in a P - and T -noninvariant interaction with matter. Hypothetical non-Newtonian gravitational interactions mediates an additional short-range potential between neutrons and bulk matter. These interactions between the neutron and the mirror of a Lloyd-type neutron interferometer cause a phase shift of neutron waves. We estimate the sensitivity and systematic effects of possible experiments.

DOI: 10.7868/S0044451013040101

1. INTRODUCTION

It is believed that the Standard model is a low-energy approximation of some more fundamental theory. Most popular extensions of the Standard Model, supersymmetric and superstring theories, predict the existence of new particles and hence new interactions. These new particles were not detected up to now because of their too large mass, or too weak interaction with ordinary matter. This last case is of interest in our discussion of a search for new hypothetical weak interactions of a different nature.

The possible existence of new interactions with macroscopic ranges and weak coupling to matter currently attracts increasing attention. A large number of experiments have been performed to search for new forces in a wide range of distance scales. Here, we consider the possibilities of the neutron Lloyd's mirror interferometer in searching for some of these new interactions.

The Lloyd's mirror interferometer (Fig. 1), well known in the light optics, has not yet been discussed in the experimental neutron optics.

The geometric phase shift is determined by the difference of path lengths of the reflected and nonreflected beams:

$$\begin{aligned} \varphi_{geom} &= \varphi_{II,geom} - \varphi_{I,geom} = \\ &= k \left[\sqrt{L^2 + (b+a)^2} - \sqrt{L^2 + (b-a)^2} \right] \approx 2kab/L, \quad (1) \end{aligned}$$

where k is the neutron wave vector, L , b and a are given in the Fig. 1 caption. The last equality is valid with the relative precision better than ab/L^2 . The geometric phase shift linearly depends on the interference coordinate b . This means that the interference pattern $I \propto \sin^2(\pi ab/\lambda_n L)$ in the absence of any potentials is sinusoidal with high precision $ab/L^2 \sim 10^{-8}$ at $a \sim b \sim 10^{-2}$ cm and $L = 1$ m. The period of oscillations in the interference pattern is $\Lambda_{osc} = \lambda_n L/2a$, where λ_n is the neutron wavelength, and is approximately $1 \mu\text{m}$ for the energy range of thermal neutrons and reasonable parameters of the interferometer. But for very cold neutrons in the μeV -energy range, the period of the interference oscillations approaches dozens of μm , and an interference picture can be registered with a narrow (about $1 \mu\text{m}$) slit at a detector window or with modern high-resolution position-sensitive neutron detectors.

The idea of a possible application of the Lloyd's mirror interferometer for the search for new hypothetical interactions between matter and particles consists in measuring the neutron wave phase shift produced by a hypothetical mirror–neutron potential. We here consider three actively discussed hypothetical interactions: the cosmological scalar fields proposed to explain the accelerated expansion of the Universe, the axion-like

*E-mail: pokot@nf.jinr.ru

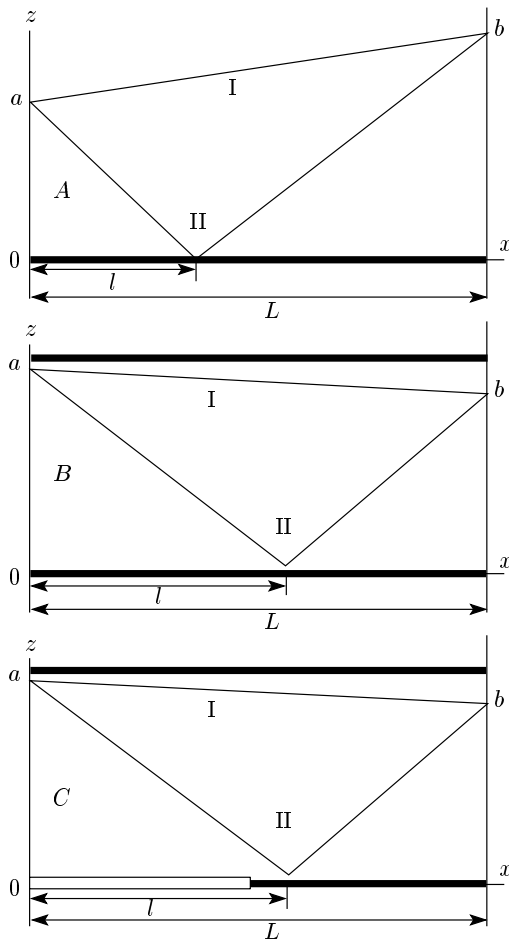


Fig. 1. Three possible configurations of the neutron Lloyd's mirror interferometer: (A) the standard Lloyd's mirror geometry; (B) interferometer with two mirrors, only the bottom one is reflecting; (C) the length of the reflecting mirror is decreased twice to avoid multiple reflections. All planes are vertical, and hence the effect of gravity on interference is reduced. The height of the slit above the reflecting plane is a , L is the distance from the slit to the detector surface, b is the distance of the detector coordinate from the reflecting plane, $l = aL/(a + b)$ is the x coordinate of the beam-II reflection point from the mirror

spin-dependent pseudoscalar nucleon–nucleon and/or nucleon–electron interaction, and hypothetical deviation of the gravitation law from the Newtonian one at small distances (non-Newtonian gravity).

2. CHAMELEON SCALAR FIELD

There is evidence of the accelerated expansion of the Universe. The nature of this effect is one of the

most exciting problems in physics and cosmology. It is not yet clear whether the explanation of the fact that gravity becomes repulsive at large distances should be found within general relativity or within a new theory of gravitation. One possibility to explain this fact is to modify the general relativity theory, and there are a number of proposals of this kind. Among various ideas proposed to explain this astronomical observation in an alternative way, one of popular variants is a new matter component of the Universe, a cosmological scalar field of the quintessence type [1] dominating the present-day density of the Universe (see [2, 3] for the recent reviews).

Acting at cosmological distances, the mass of this field should be of the order of the Hubble constant: $\hbar H_0/c^2 = 10^{-33} \text{ eV}/c^2$.

The massless scalar fields appearing in string and supergravity theories couple to matter with gravitational strength. Because of the direct coupling to matter with the strength of gravity, the existence of light scalar fields leads to a major violation of the equivalence principle. In the absence of self-interaction of the scalar field, the experimental constraints on such a field are very strict, requiring its coupling to matter to be unnaturally small.

The solution proposed in Refs. [4–9] consists in the introduction of the coupling of the scalar field to matter of such a form that as a result of self-interaction and the interaction of the scalar field with matter, the mass of the scalar field depends on the local matter environment.

In the proposed variant, the coupling to matter is of the order of one expected from string theory, but is very small on cosmological scales. In the environment of the high matter density, the mass of the field increases, the interaction range strongly decreases, and the equivalence principle is not violated in laboratory experiments for the search for the long-range fifth force. The field is confined within the matter that screens its existence from the external world. In this way, the chameleon fields evade tests of the equivalence principle and the fifth force experiments even if these fields are strongly coupled to matter. As a result of the screening effect, the laboratory gravitational experiments are unable to set an upper limit on the strength of the chameleon–matter coupling.

The deviations of results of measurements of gravity forces at macroscopic distances from calculations based on Newtonian physics can be seen in the experiments of Galileo, Eötvös or Cavendish type [10] performed with macro-bodies. At smaller distances (10^{-7} – 10^{-2}) cm, the effect of these forces can be observed

in measurements of the Casimir force between closely placed macro-bodies (see [11] for a review) or in the atomic force microscopy experiments. Casimir force measurements may to some degree evade the screening and probe the interactions of the chameleon field at the micrometer range despite the presence of the screening effect [9, 12, 13].

At even smaller distances, such experiments are not sensitive enough, and high-precision particle scattering experiments may play their role. In view of the absence of electric charge, experiments with neutrons are more sensitive than with charged particles; electromagnetic effects in scattering of neutrons by nuclei are generally known and can be accounted for with high precision [14, 15].

As regards the chameleon interaction of elementary particles with bulk matter, it was mentioned in [16] that a neutron should not show a screening effect: the chameleon-induced interaction potential of bulk matter with neutron can be observed. It was also proposed in [16] to search for a chameleon field through the energy shift of ultracold neutrons in the vicinity of a reflecting horizontal mirror. From the already performed experiments on the observation of gravitational levels of neutrons, the constraints on parameters characterizing the strength of chameleon-matter interaction were obtained in [16].

Chameleons can also couple to photons. It was proposed in [17, 18] to search in a closed vacuum cavity for the afterglow effect resulting from the chameleon-photon interaction in a magnetic field. The GammeV-CHASE [19, 20] and ADMX [21] experiments based on this approach are intended to measure (constrain) the coupling of the chameleon scalar field to matter and photons.

In the approach proposed here only, the chameleon-matter interaction is measured, irrespective of the existence of the chameleon-photon interaction. The approach is based on the standard method of measuring the phase shift of a neutron wave in the interaction potential.

Irrespective of any particular variant of the theory, testing the interaction of particles with matter at small distances may be interesting.

In one of popular variants of the chameleon scalar field theory [4–9], the chameleon effective potential is

$$V_{eff}(\phi) = V(\phi) + \exp(\beta\phi/M_{Pl})\rho, \quad (2)$$

where

$$V(\phi) = \Lambda^4 + \frac{\Lambda^{4+n}}{\phi^n} \quad (3)$$

is the scalar field potential, M_{Pl} is the Planck mass, ρ is the local energy density of the environment, $\Lambda = (\hbar^3 c^3 \rho_{d.e.})^{1/4} = 2.4 \text{ meV}$ is the dark energy scale, $\rho_{d.e.} \approx 0.7 \cdot 10^{-8} \text{ erg/cm}^3$ is the dark energy density, and β is the interaction parameter not predicted by the theory.

The chameleon interaction potential of a neutron with bulk matter (mirror) was calculated in [16]:

$$\begin{aligned} V(z) &= \beta \frac{m}{M_{Pl}\lambda} \left(\frac{2+n}{\sqrt{2}}\right)^{2/(2+n)} \left(\frac{z}{\lambda}\right)^{2/(2+n)} = \\ &= \beta \cdot 0.9 \cdot 10^{-21} \text{ eV} \left(\frac{2+n}{\sqrt{2}}\right)^{2/(2+n)} \left(\frac{z}{\lambda}\right)^{2/(2+n)} = \\ &= V_0 \left(\frac{z}{\lambda}\right)^{2/(2+n)}, \quad (4) \end{aligned}$$

$$V_0 = \beta \cdot 0.9 \cdot 10^{-21} \text{ eV} \left(\frac{2+n}{\sqrt{2}}\right)^{2/(2+n)}, \quad (5)$$

where $\lambda = \hbar c/\Lambda = 82 \mu\text{m}$ and m is the neutron mass.

To reduce the strong effect of Earth's gravity, the mirror of the interferometer is vertical. The neutron wave vector k' in potential V is

$$k'^2 = k^2 - \frac{2mV}{\hbar^2}, \quad k' = k - \frac{mV}{\hbar k}. \quad (6)$$

The phase shift due to the chameleon-mediated interaction potential of a neutron with the mirror, depending on the distance from the mirror, is obtained by integration along trajectories $\varphi = \oint k' ds = \varphi_{II} - \varphi_{I}$, where φ_I and φ_{II} are the phases obtained along trajectories I and II (see Fig. 1):

$$\begin{aligned} \varphi_I &= k\sqrt{L^2 + (b-a)^2} - \frac{mV_0\sqrt{1 + (b-a)^2/L^2}}{k\hbar^2\lambda^{\alpha_n-1}} \times \\ &\times \int_0^L \left(a + \frac{b-a}{L}x\right)^{\alpha_n-1} dx = \\ &= \varphi_{I,geom} - \frac{\gamma\sqrt{1 + [(b-a)/L]^2}}{\lambda^{\alpha_n-1}\alpha_n(b-a)} (b^{\alpha_n} - a^{\alpha_n}), \quad (7) \end{aligned}$$

$$\begin{aligned} \varphi_{II} &= k\sqrt{L^2 + (b+a)^2} - \frac{mV_0\sqrt{1 + (b+a)^2/L^2}}{k\hbar^2\lambda^{\alpha_n-1}} \times \\ &\times \left[\int_0^l \left(a - \frac{b+a}{L}x\right)^{\alpha_n-1} dx + \right. \\ &\left. + \int_l^L \left(\frac{b+a}{L}x - a\right)^{\alpha_n-1} dx \right] = \\ &= \varphi_{II,geom} + \frac{\gamma\sqrt{1 + (b+a)^2/L^2}}{\lambda^{\alpha_n-1}\alpha_n(b+a)} (b^{\alpha_n} + a^{\alpha_n}). \quad (8) \end{aligned}$$

Here, $l = aL/(a + b)$ is the x coordinate of the beam-II reflection point from the mirror, $\gamma = mV_0L/k\hbar^2$, and $\alpha_n = (4 + n)/(2 + n)$.

The phase shift from the chameleon neutron-mirror potential is

$$\begin{aligned} \varphi_{cham} &= \varphi_{II,cham} - \varphi_{I,cham} = \\ &= \frac{\gamma}{\lambda^{\alpha_n-1}\alpha_n} \left[\frac{b^{\alpha_n} - a^{\alpha_n}}{b - a} \sqrt{1 + \frac{(b - a)^2}{L^2}} - \right. \\ &\quad \left. - \frac{b^{\alpha_n} + a^{\alpha_n}}{b + a} \sqrt{1 + \frac{(b + a)^2}{L^2}} \right] \approx \\ &\approx \frac{\gamma}{\lambda^{\alpha_n-1}\alpha_n} 2ab \frac{b^{\alpha_n-1} - a^{\alpha_n-1}}{b^2 - a^2}. \end{aligned} \quad (9)$$

For a nonstrictly vertical mirror, the component of the Earth's gravity normal to the surface of the mirror produces the potential $V_{gr} = \varkappa mgz$, where g is the acceleration of gravity and the coefficient \varkappa depends on the angle θ between the gravity vector and the mirror plane. At $\theta = 10''$, we have $\varkappa \approx 5 \cdot 10^{-5}$. This linear potential leads to the additional phase shift

$$\begin{aligned} \varphi_{gr} &= \varphi_{II,gr} - \varphi_{I,gr} = \frac{\varkappa gm^2}{2k\hbar^2(a + b)} \times \\ &\times \left[(b + a)^2 \sqrt{L^2 + (b - a)^2} - \right. \\ &\quad \left. - (b^2 + a^2) \sqrt{L^2 + (b + a)^2} \right] \approx \frac{\varkappa gm^2}{k\hbar^2} \frac{abL}{a + b}, \end{aligned} \quad (10)$$

calculated in analogy with Eqs. (6)–(9).

The Coriolis phase shift due to Earth's rotation [22] is

$$\varphi_{Cor} = \frac{2m}{\hbar} (\mathbf{\Omega} \cdot \mathbf{A}), \quad (11)$$

where $\mathbf{\Omega}$ is the vector of angular rotation of Earth and \mathbf{A} is the vector of the area enclosed by the interferometer beams.

With $A = abL/(a + b)$, for the location of the Institute Laue-Langevin (where a good very cold neutron source has been constructed [23]), we have

$$\varphi_{Cor} = \frac{0.16abL}{a + b} \text{ rad},$$

where a , b , and L are expressed in centimeters. As expected, it is similar to the gravitational phase shift in its dependence on both the slit and the interference coordinates.

We must also calculate the phase shift of the neutron wave along beam II at the point of reflection. Neglecting the imaginary part of the potential of the mirror, we write the amplitude of the reflected wave as $r = \exp(-i\varphi_{refl})$ with the phase

$$\varphi_{refl} = 2 \arccos(k_{\perp}/k_b) \approx \pi - \delta\varphi_{refl}, \quad (12)$$

where

$$\delta\varphi_{refl} = 2 \frac{k_{\perp}}{k_b} \approx \pi - 2 \frac{k}{k_b} \frac{a + b}{L}, \quad (13)$$

k_{\perp} is the neutron wave vector component normal to the mirror surface, and k_b is the boundary wave vector of the mirror. This phase shift linearly depends on b , similarly to the geometric phase shift φ_{geom} .

The reflected and nonreflected beams follow slightly different paths in the interferometer. Therefore, in the vertical arrangement of the reflecting mirror, they spent different times in Earth's gravitational field, with $\Delta t = 2ab/Lv$, where v is the neutron velocity. The difference in vertical shifts of the reflected and nonreflected beams is $\Delta h = 2gab/v^2$, and the phase shift due to this difference is

$$\Delta\varphi_{vert} = kg^2abL/v^4. \quad (14)$$

With our parameters of the interferometer, this value is of the order of 10^{-4} .

The total measured phase shift is

$$\varphi = \varphi_{geom} + \varphi_{cham} + \varphi_{gr} + \varphi_{Cor} + \varphi_{refl}. \quad (15)$$

The gravitational phase shift can be suppressed by installing the mirror vertically with the highest possible precision. On the other hand, the gravitational phase shift may be used for calibration of the interferometer by rotation around the horizontal axis. The phase shifts due to Earth's rotation φ_{Cor} and reflection φ_{refl} may be calculated and taken into account in the analysis of the interference curve.

Figure 2 shows the calculated phase shift φ_{cham} for an idealized Lloyd's mirror interferometer (strictly monochromatic neutrons, the width of the slit is zero, the detector resolution is perfect), the gravitational phase shift φ_{gr} at $\varkappa = 5 \cdot 10^{-5}$ (the deviation of the mirror from verticality is $10''$), and $\delta\varphi_{refl}$ ($k_b = 10^6 \text{ cm}^{-1}$).

It is essential that the sought phase shift due to hypothetical chameleon potential depends on the interference coordinate nonlinearly. The effect of the hypothetical interaction has to be inferred from analysis of the interference pattern after subtracting the effects of Earth's gravity, Coriolis force, and reflection.

Figure 3 demonstrates the calculated interference pattern for the same parameters of the interferometer as in Fig. 2 for two cases: (1) with the geometrical phase shift φ_{geom} , the gravitational phase shift φ_{gr} at $\varkappa = 5 \cdot 10^{-5}$, and the phase shift of ray II at reflection $\delta\varphi_{refl} = \pi - \varphi_{refl}$ ($k_b = 10^6 \text{ cm}^{-1}$) taken into account;

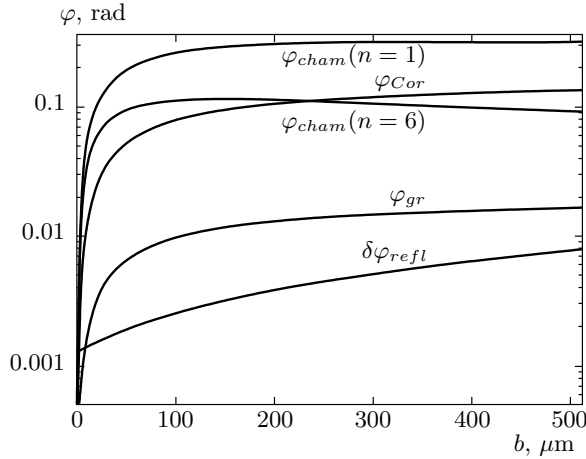


Fig. 2. The neutron wave phase shifts φ_{cham} in the Lloyd's mirror interferometer with the neutron wave length $\lambda_n = 100 \text{ \AA}$ (the neutron velocity $v = 40 \text{ m/s}$), $L = 1 \text{ m}$, and $a = 100 \text{ \mu m}$, and with the interaction parameters of the chameleon field with matter $\beta = 10^7$, $n = 1$, and $n = 6$. Also shown: the gravitational phase shift φ_{gr} at $\varkappa = 5 \cdot 10^{-5}$; the Coriolis phase shift φ_{Cor} , and the effect of reflection $\delta\varphi_{refl} = \pi - \varphi_{refl}$ at $k_b = 10^6 \text{ cm}^{-1}$. The period of oscillations in the interference pattern is $\Lambda_{osc} = \lambda_n L / 2a = 50 \text{ \mu m}$

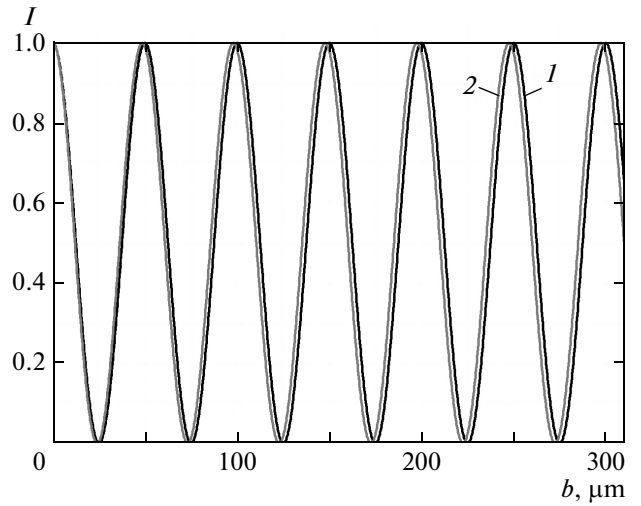


Fig. 3. The calculated interference pattern for the neutron–mirror interaction via the chameleon field (the parameters of the interferometer are the same as in Fig. 2): (1) the geometrical phase shift φ_{geom} the gravitational phase shift φ_{gr} at $c = 5 \cdot 10^{-5}$, and the phase shift of the ray II at reflection $\delta\varphi_{geom}$ the gravitation phase shift φ_{gr} at $c = 5 \cdot 10^{-5}$, and the phase shift of the ray II at reflection $\delta\varphi_{refl} = \pi - \varphi_{refl}$ ($k_b = 10^6 \text{ cm}^{-1}$) are taken account; (2) the same plus the phase shift due to the chameleon field with the matter interaction parameters $\beta = 10^7$ and $n = 1$

(2) the same plus the phase shift due to the chameleon field with the matter interaction parameters $\beta = 10^7$ and $n = 1$.

After subtracting all the phase shifts except the purely geometrical one, the interference pattern should be strongly sinusoidal with the period of oscillations determined by the geometric phase shift: $\Lambda_{osc} = \lambda_n L / 2a$. The number of oscillations in the interference pattern with the coordinate less than b is $n_{osc} = 2ab / \lambda_n L$.

It follows from these calculations that the effect of the chameleon interaction of a neutron with matter may be tested in the strong-coupling range with the interaction parameter down to $\beta \sim 10^7$ or lower.

The existing constraints on the parameters β and n can be found in Fig. 1 in Ref. [16]. For example, the allowed range of parameters for the strong-coupling regime $\beta \gg 1$ are $50 < \beta < 5 \cdot 10^{10}$ for $n = 1$, $10 < \beta < 2 \cdot 10^{10}$ for $n = 2$, and $\beta < 10^{10}$ for $n > 2$. It can be seen that Lloyd's mirror interferometer may be able to constrain the chameleon field in a large domain of the coupling parameters.

3. AXION-LIKE SPIN-DEPENDENT INTERACTION

There are general theoretical indications of the existence of interactions coupling mass to particle spin [24–28]. Experimental search for these forces is a promising way to discover new physics.

On the other hand, a number of concrete proposals were published of new light, scalar or pseudoscalar, vector or pseudovector weakly interacting bosons. The masses of these new hypothetical particles and their coupling to nucleons, leptons, and photons are not predicted by the proposed models.

The popular solution of the strong CP problem is the existence of a light pseudoscalar boson — the axion [29]. The axion coupling to fermions has the general form $g_{aff} = C_f m_f / f_a$, where C_f is a model-dependent factor. Here, f_a is the Peccei–Quinn symmetry breaking scale, which is not predicted, and hence the axion may a priori have a mass in a very wide range, $10^{-12} \text{ eV} < m_a < 10^6 \text{ eV}$. The main part of this mass range from both low and high mass boundaries was excluded as a result of numerous experiments and constraints from astrophysical considerations [30]. Astro-

physical bounds are based on some assumptions concerning the axion and photon fluxes produced in stellar plasma.

More recent constraints limit the axion mass to $10^{-5} \text{ eV} < m_a < 10^{-3} \text{ eV}$ with accordingly very small coupling constants to quarks and photons [30].

The axion is one of the best candidates for the cold dark matter of the Universe [31, 32].

Axions can mediate a P - and T -reversal violating monopole–dipole interaction potential between spin and matter (polarized and unpolarized nucleons or electrons) [33]:

$$V_{mon-dip}(\mathbf{r}) = g_s g_p \frac{\hbar^2 \boldsymbol{\sigma} \cdot \mathbf{n}}{8\pi m_n} \left(\frac{1}{\lambda r} + \frac{1}{r^2} \right) e^{-r/\lambda}, \quad (16)$$

where g_s and g_p are dimensionless coupling constants of the scalar and pseudoscalar vertices (unpolarized and polarized particles), m_n is the nucleon mass at the polarized vertex, $s = \hbar \boldsymbol{\sigma} / 2$ is the nucleon spin, $\boldsymbol{\sigma}$ is the Pauli matrix, r is the distance between the nucleons, $\lambda = \hbar / m_a c$ is the range of the force, m_a is the axion mass, and $\mathbf{n} = \mathbf{r} / r$ is a unit vector.

Several laboratory searches (mostly by the torsion pendulum method) provided constraints on the product of the scalar and pseudoscalar couplings at macroscopic distances $\lambda > 10^{-2} \text{ cm}$ (see reviews [34–37]).

There are also experiments on the search for the monopole–dipole interactions in which the polarized probe is an elementary particle: a neutron [38–41] or atoms and nuclei [42, 43] (see the correction in [44]).

For the monopole–monopole interaction due to exchange by a pseudoscalar boson [33],

$$V_{mon-mon}(r) = \frac{g_s^2}{4\pi} \frac{\hbar c}{r} e^{-r/\lambda}, \quad (17)$$

the limit on the scalar coupling constant g_s can be inferred from the experimental search for the “fifth force” in the form of the Yukawa-type gravity potential $U_5(r) = \alpha_5 G M m e^{-r/\lambda} / r$:

$$g_s^2 = \frac{4\pi G m_n^2 \alpha_5}{\hbar c} \approx 10^{-37} \alpha_5, \quad (18)$$

where α_5 is the “fift-force” Yukawa-type coupling constant.

It follows from the experimental tests of gravitation at small distances (see reviews in [34, 35]) that g_s^2 is limited by a value $10^{-40} - 10^{-38}$ in the interaction range $1 \text{ cm} > \lambda > 10^{-4} \text{ cm}$. The sensitivity of these experiments decreases with decreasing the interaction range below approximately 1 cm.

The pseudoscalar coupling constant is restricted by $g_p < 10^{-9}$ from astrophysical considerations [37, 45].

It follows that the constraints obtained and expected from further laboratory searches are weak compared to the limit on the product $g_s g_p < 10^{-28}$ inferred from the above-mentioned separate constraints on g_s and g_p . Although laboratory experiments may not lead to bounds that are strongest numerically, measurements made in terrestrial laboratories produce the most reliable results. The direct experimental constraints on the monopole–dipole interaction may be useful for limiting a more general class of low-mass bosons irrespective of any particular theoretical model. In what follows, the constraint on the product $g_s g_p$ may be used for the limits on the coupling constant of this more general interaction.

It follows from (16) that the potential between the layer of substance and a nucleon separated by the distance x from the layer surface is

$$V_{mon-dip}(x) = \pm g_s g_p \frac{\hbar^2 N \lambda}{4m_n} (e^{-x/\lambda} - e^{-(x+d)/\lambda}) = \pm V_0 e^{-x/\lambda} \quad (d \gg \lambda), \quad (19)$$

where $V_0 = g_s g_p \hbar^2 N \lambda / 4m_n$, N is the nucleon density in the layer, and d is the layer thickness. The “+” or “−” depends on the nucleon spin projection on x axis (the surface normal).

Phase shifts of beams I and II due to the interaction in Eq. (19) are calculated similarly to Eqs. (7) and (8):

$$\begin{aligned} \varphi_I &= k \sqrt{L^2 + (b-a)^2} + \frac{mV_0}{k\hbar^2 L} \sqrt{L^2 + (b-a)^2} \times \\ &\times \int_0^L \exp \left[-\frac{1}{\lambda} \left(a + \frac{b-a}{L} x \right) \right] dx = \varphi_{I,geom} + \\ &+ \frac{mV_0}{k\hbar^2} \sqrt{L^2 + (b-a)^2} \frac{\lambda}{b-a} (e^{-a/\lambda} - e^{-b/\lambda}) = \\ &= \varphi_{I,geom} + \varphi_{I,pot} \quad (20) \end{aligned}$$

and

$$\begin{aligned} \varphi_{II} &= k \sqrt{L^2 + (b+a)^2} + \frac{mV_0}{k\hbar^2 L} \sqrt{L^2 + (b+a)^2} \times \\ &\times \left[\int_0^l \exp \left[-\frac{1}{\lambda} \left(a - \frac{b+a}{L} x \right) \right] dx + \right. \\ &\left. + \int_l^L \exp \left[-\frac{1}{\lambda} \left(\frac{b+a}{L} x - a \right) \right] dx \right] = \\ &= \varphi_{II,geom} + \frac{mV_0}{k\hbar^2} \sqrt{L^2 + (b+a)^2} \frac{\lambda}{b+a} \times \\ &\times (2 - e^{-a/\lambda} - e^{-b/\lambda}) = \varphi_{II,geom} + \varphi_{II,pot}. \quad (21) \end{aligned}$$

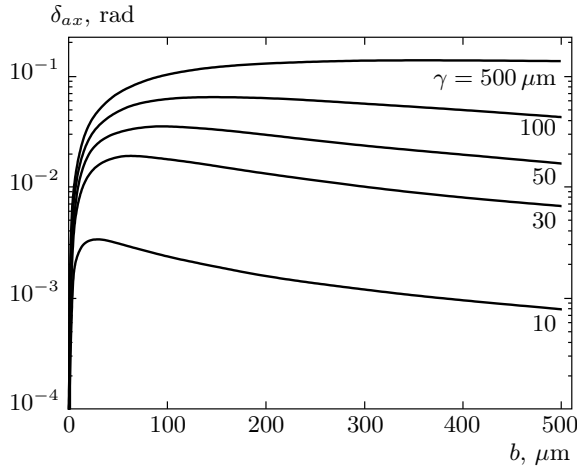


Fig. 4. The neutron wave phase shift δ_{ax} at different interaction ranges λ of the axion-like spin-dependent interaction with the product of the coupling constants $g_s g_p = 10^{-18}$. Lloyd's mirror interferometer has the same parameters as in Fig. 2

For the spin-dependent potential in Eq. (19), the signs of the potential V_0 and, accordingly, the phase shift φ_{pot} are opposite for the two spin orientations with respect to the mirror surface normal. The difference in these phase shifts, measured in the experiment, is

$$(\varphi_I^+ - \varphi_{II}^+) - (\varphi_I^- - \varphi_{II}^-) = 2(\varphi_I - \varphi_{II}) = \delta\varphi. \quad (22)$$

The geometric, gravitational phase shifts and the phase shift of beam II at reflection calculated previously are independent of spin.

The phase shift due to the axion interaction is

$$\varphi_{ax} = \frac{2\gamma\lambda a}{b^2 - a^2} \left[(1 - e^{-b/\lambda}) - b(1 - e^{-a/\lambda}) \right], \quad (23)$$

where $\gamma = g_s g_p N \lambda L / 4k$. For $b = a$ and $\lambda/a \ll 1$, we have $\varphi_{ax} \rightarrow \gamma\lambda/a$.

Figure 4 shows the neutron wave phase shift φ_{ax} for different interaction ranges λ . Lloyd's mirror interferometer has the following parameters: neutron wave length 100 \AA (neutron velocity $v = 40 \text{ m/s}$), $L = 1 \text{ m}$, $a = 100 \text{ }\mu\text{m}$, and the interaction strength $g_s g_p = 10^{-18}$. The possible sensitivity seen from this figure shows that constraints on the monopole-dipole interaction that can be obtained with the method of the neutron Lloyd's mirror interferometry are competing with the best constraints currently obtained by other methods (see Ref. [37]).

Figure 5 shows the calculated interference pattern due to an axion-like spin-dependent interaction. The gradient of the external magnetic field $\nabla(\boldsymbol{\mu}_n \cdot \mathbf{B})$ normal to the mirror plane ($\boldsymbol{\mu}_n$ is the neutron magnetic

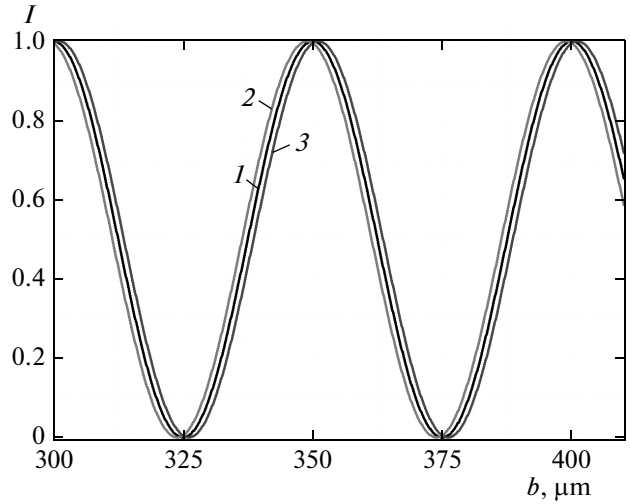


Fig. 5. Calculated interference pattern due to an axion-like spin-dependent interaction with $g_s g_p = 10^{-18}$ and the interaction range $\lambda = 500 \text{ }\mu\text{m}$ (the interferometer has the same parameters as in Fig. 2): (1) $V_{mon-dip} = 0$; (2) spin up; (3) spin down

moment) may produce the phase shift effect on polarized neutrons, similar to the effect of the gravitational force $F_{gr} = mg$ (see Eq. (10)). Simple calculation gives that the magnetic field gradient 0.01 Oe/cm is equivalent to approximately $5 \cdot 10^{-5}$ of Earth's gravitation.

A significant increase in sensitivity may be achieved in the range of small λ ($\lambda/a \ll 1$) if the geometry shown in Fig. 1B is used, where the slit is located in close vicinity to the surface of an additional (upper) nonreflecting mirror. The axion-like potential is produced in this case by both mirrors, but with opposite signs in accordance with Eq. (19).

To avoid multiple reflections, the boundary wave vector of the reflecting mirror must satisfy the condition $k_b \leq 2ka/L$, or the neutron beam incident on the slit must be collimated such that the first half of the reflecting mirror is not illuminated by the neutrons. In this geometry, the phase shift due to the axion-like monopole-dipole interaction of the neutron with both mirrors is

$$\varphi_{ax} = \frac{2\gamma\lambda a}{b^2 - a^2} \left[e^{(b-a)/\lambda} - e^{-a/\lambda} + e^{-b/\lambda} - 1 \right]. \quad (24)$$

In this case, $\varphi_{ax} \rightarrow \gamma(1 - e^{-a/\lambda}) \rightarrow \gamma$ as $b \rightarrow a$ for $\lambda/a \ll 1$ compared to $\gamma\lambda/a$ in the case of one mirror (Eq. (23)).

The gain in sensitivity at $\lambda/a \ll 1$ compared to the case in Fig. 4 is illustrated in Fig. 6.

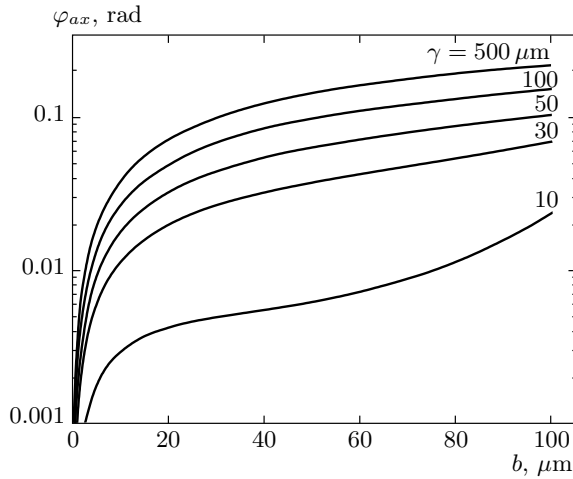


Fig. 6. Neutron wave phase shift φ_{ax} at different interaction ranges λ of the axion-like spin-dependent interaction with the product of the coupling constants $g_s g_p = 10^{-18}$. Lloyd’s mirror interferometer has the geometry shown in Fig. 1B with the same parameters as in Fig. 2, and the distance between mirrors 100 μm

4. NON-NEWTONIAN GRAVITY

New short-distance spin-independent forces are frequently predicted in theories extending the Standard Model. These interactions can violate the equivalence principle if they depend on the composition of bodies or the type of particles.

Precision experiments to search for deviations from Newton’s inverse square law and for violation of the weak equivalence principle have been performed in a number laboratories (reviews can be found in [10, 34–37]).

The pioneering ideas of multidimensional models first formulated in the first half of the XXth century (G. Nordström, T. Kaluza, and O. Klein) received renewed interest in [46–48, 50]. The development of supergravity and superstring theories required extra dimensions for their consistency. A more recent promising development contained in [49–53] proposed mechanisms in which the standard model fields are located on the 4-dimensional brane while gravity propagates to the $(4 + n)$ -bulk with a larger number of dimensions. As a result, the gravitational law may be different from the Newtonian one.

The frequently used parameterization of a new spin-independent hypothetical short-range interaction potential has the Yukawa-type form

$$U_{Yuk}(r) = \frac{\alpha G M m}{r} e^{-r/\lambda}, \quad (25)$$

where G is the Newtonian gravitational constant, M and m are the masses of gravitating bodies, α is a dimensionless parameter characterizing the strength of the new force relative to gravity, and $\lambda = \hbar/m_0 c$ is the Compton wavelength of the particle with the mass m_0 . The mass m_0 can be the mass of the new scalar field responsible for the short-range interaction. In this case, $\alpha \sim g_s^2$ is the product of the scalar coupling constants. Alternatively, m_0 can be the mass of the lightest Kaluza–Klein state (which is the leading-order mode) when the short-range interaction comes from an extra-dimensional extension of the standard model.

The strength α is constrained to be below unity for $\lambda \geq 100 \mu\text{m}$ [37, 54], but for shorter distances, the measurements are not as sensitive, being complicated by the Casimir and electrostatic forces [11]. The sensitivity reached in the experiments aiming to test spin-independent interactions between elementary particles and matter is by orders of magnitude worse: for $\lambda = 100 \mu\text{m}$, it is at the level $\alpha > 10^{11}$ [55], with the loss of sensitivity at shorter distances.

The potential following from the interaction in Eq. (25) between a layer of substance and a neutron separated by the distance x from the layer surface is

$$V_{Yuk}(x) = 2\pi\alpha m_n^2 N G \lambda^2 e^{-x/\lambda} = V_0 e^{-x/\lambda}, \quad (26)$$

where $N \approx \rho m_n$ is the nucleon density in the layer, ρ is density of the mirror, and $V_0 = 2\pi\alpha m_n^2 N G \lambda^2$ in this case.

The potential in Eq. (26) has the same coordinate dependence as the axion-like interaction potential in Eq. (19), and therefore the expressions for the phase shifts are similar to Eq. (23) with $\gamma = 2\pi\alpha\rho\lambda^2 m_n^2 L/k\hbar^2$.

Figure 7 shows the phase shifts due to the non-Newtonian interaction in Eq. (26) at the same parameters of the interferometer as in Fig. 1 and $\rho = 10 \text{ g/cm}^3$.

For the “inverted” Lloyd’s mirror geometry, when the reflecting mirror has a much lower density such that its gravitational effect is insignificant compared to the effect of the upper mirror, the phase shift is

$$\varphi_{Yuk} = \frac{2\gamma\lambda}{b^2 - a^2} \times \left[a(e^{-a/\lambda} - e^{(b-a)/\lambda}) + b(1 - e^{-a/\lambda}) \right]. \quad (27)$$

For $b \rightarrow a$ and $\lambda/a \rightarrow 0$, we have $\varphi_{Yuk} \rightarrow \gamma$, with a significant gain in sensitivity for $\lambda/a \ll 1$ compared to the geometry in Fig. 1A and Eq. (23). To avoid multiple reflections in this case, the geometry of Fig. 1C may be applied, in which the reflecting mirror has only half the length in Fig. 1A. This gain is illustrated in Fig. 8.

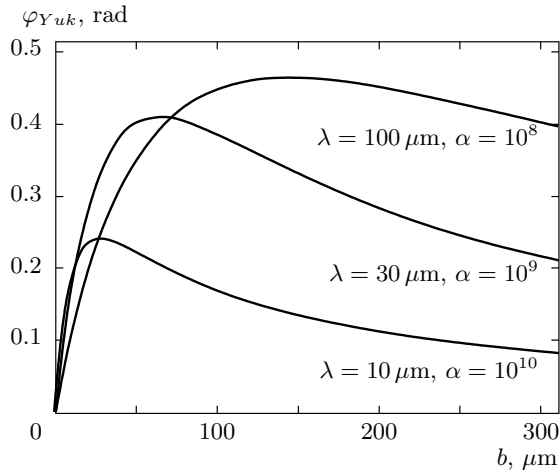


Fig. 7. The neutron wave phase shifts φ_{Yuk} in the Lloyd's mirror interferometer of the geometry shown in Fig. 1A and with the same parameters as in Fig. 2

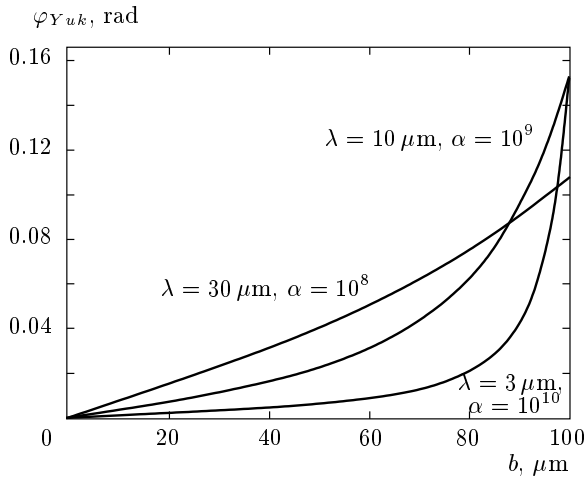


Fig. 8. The neutron wave phase shifts φ_{Yuk} in the Lloyd's mirror interferometer of the geometry shown in Fig. 1C and with the same parameters as in Fig. 2

5. FEASIBILITY

As mentioned above, the interference may be measured step by step by shifting a narrow slit with the width $\delta b \ll \Lambda_{osc}$. A better option is to use the coordinate detector measuring all the interference picture simultaneously in this way. The current spatial resolution of position-sensitive slow-neutron detectors is at the level of $5 \mu\text{m}$ with electronic registration [56] and about $1 \mu\text{m}$ with the plastic nuclear track detection technique [57]. With a ^{10}B neutron converter $1 \mu\text{m}$ thick, the registration efficiency for 100 \AA -wave-length neutrons may be close to 100%.

From Ref. [23], where the neutron phase density at the PF-2 very cold neutron (VCN) channel at the Institute Laue-Langevin was measured to be $0.25 \text{ cm}^{-3} \cdot (\text{m/s})^{-3}$ at $v = 50 \text{ m/s}$, it is possible to estimate the VCN flux density as $\phi_{VCN} = 1.66 \cdot 10^5 \text{ cm}^{-2} \cdot \text{s}^{-1} \cdot (\text{m/s})^{-1} \approx 1 \cdot 10^5 \text{ cm}^{-2} \cdot \text{s}^{-1} \cdot \text{ \AA}^{-1}$ (for the boundary velocity 6.5 m/s of the neutron guide). On the other hand, Ref. [58] gives the larger value $\phi_{VCN} = 4 \cdot 10^5 \text{ cm}^{-2} \cdot \text{s}^{-1} \cdot (\text{m/s})^{-1}$ for the same channel.

Using the Zernike theorem, it is possible to calculate the width d of the slit necessary to satisfy good coherence within the coherence aperture ω , i.e., the maximum angle between diverging interfering beams: $x = \pi\omega d_{sl}/\lambda_n \leq 1$, if the slit is irradiated with an incoherent neutron flux. With $\omega = 2b_{max}/L$, the slit width $d_{sl} \leq L\lambda_n/2\pi b_{max} \approx 2 \mu\text{m}$ for $b_{max} = 1 \text{ mm}$ (20 orders of interference at the period of interference $\Lambda_{osc} = \lambda_n L/2a = 50 \mu\text{m}$ at $a = 100 \mu\text{m}$).

For the monochromaticity 5 \AA (the coherence length $l_{coh} = 20\lambda_n$), the slit width $2 \mu\text{m}$ and length 3 cm , the divergence of the incident beam is determined by the VCN guide boundary velocity 6.5 m/s : $\Omega = 6.5/100 = 0.065$, the interference aperture $\omega = 2b/L = 0.2/100 = 2 \cdot 10^{-3}$, and hence $\omega/\Omega = 0.03$, the count rate to all interference curves with a width of 1 mm (20 orders of interference) is given by $10^5 \cdot 5 \cdot (2 \cdot 10^{-4}) \cdot 3 \cdot 0.03 \sim 10 \text{ s}^{-1}$. In one-day measurements, the number of events in one period of interference is about $4 \cdot 10^4$. It is enough to observe the phase shift of approximately 0.1 corresponding to the effect at $\beta = 10^7$.

Distinctive feature of the Lloyd's mirror interferometer is the possibility to register all the interference pattern simultaneously along the z coordinate starting from $z = 0$ (see Fig. 1). The measured interference pattern is then analyzed as regards the presence of the sought effects, after taking the known corrections for gravity, Coriolis, and reflection phase shifts into account.

The LLL-type interferometers [59, 60] may be used in principle to search for new hypothetical interactions by placing a piece of matter in the vicinity of interfering beams. But geometry of these interferometers does not permit probing hypothetical short-range interactions, the axion-like or non-Newtonian gravity, in this way.

We can estimate the sensitivity of the LLL-type interferometer to the chameleon potential, which is actually not short-range. The phase shift in this case is

$$\varphi_{LLL} = \frac{2\gamma\sqrt{1+(2a/L)^2}}{\lambda^{\alpha_n-1}}(2a)^{\alpha_n-1}, \quad (28)$$

where a is the half distance between the beams of the LLL interferometer. The sensitivity of the Lloyd's mirror and the LLL interferometers is determined by the factor $La^{\alpha n-1}/k$, which is much in favor of the Lloyd's mirror interferometer.

In LLL-type interferometers [59, 60], an interference pattern is obtained point by point by rotation of a phase flag introduced into the beams. In the case of the VCN three-grating interferometers (see, e.g., [61–63]), the phase shift between the beams is realized by the same method or by shifting the position of the grating.

The neutron Lloyd's mirror experiments may be performed with monochromatic very cold neutrons or in the time-of-flight mode using a large wavelength range, for example, 80–120 Å. The pseudorandom modulation [64, 65] is used in the correlation time-of-flight spectrometry. It was realized in the range of very low neutron energies [66]. In this case, a two-dimensional interference coordinate–time-of-flight registration gives a significant statistical gain.

As in the VCN interferometers based on three gratings, the space between the beams in the Lloyd's mirror neutron interferometer, is small (fractions of millimeters). Therefore, it can hardly be used in experiments where some devices are introduced in the beams or between the beams (for example, to investigate nonlocal quantum mechanical effects). But it may be applicable to search for short-range interactions when they are produced by a reflecting mirror.

The Lloyd's mirror neutron interferometer may be useful in a search for interactions proposed in other recently developed theories of scalar fields where the screening mechanism may be essential: symmetron [67–70] and galileon [71–79]. A more detailed consideration of the effects that may be produced by these interactions on neutron waves in the Lloyd's mirror interferometer is beyond the scope of this paper.

The author is indebted to the anonymous referee for his or her comments on the first version of the manuscript and suggestions.

REFERENCES

1. B. Ratra and P. J. E. Peebles, *Phys. Rev. D* **37**, 3406 (1988).
2. P. J. E. Peebles and B. Ratra, *Rev. Mod. Phys.* **75**, 559 (2003).
3. E. J. Copeland, M. Sami, and S. Tsujikawa, *Int. J. Mod. Phys. D* **15**, 1553 (2006).
4. J. Khoury and A. Weltman, *Phys. Rev. Lett.* **93**, 171104 (2004); *Phys. Rev. D* **69**, 044026 (2004).
5. P. Brax, C. van de Bruck, A.-C. Davis, J. Khoury, and A. Weltman, *Phys. Rev. D* **70**, 123518 (2004).
6. S. S. Gubser and J. Khoury, *Phys. Rev. D* **70**, 104001 (2004).
7. A. Upadhye, S. S. Gubser, and J. Khoury, *Phys. Rev. D* **74**, 104024 (2006).
8. D. F. Mota and D. S. Shaw, *Phys. Rev. Lett.* **97**, 151102 (2006).
9. D. F. Mota and D. S. Shaw, *Phys. Rev. D* **75**, 063501 (2007).
10. E. Fischbach and C. L. Talmadge, *The Search for Non-Newtonian Gravity*, Springer-Verlag, New-York (1998).
11. M. Bordag, U. Mohideen, and V. M. Mostepanenko, *Phys. Rep.* **353**, 1 (2001).
12. P. Brax, C. van de Bruck, A. C. Davis, D. F. Mota, and J. Shaw, *Phys. Rev. D* **76**, 124034 (2007).
13. P. Brax, C. van de Bruck, A. C. Davis, D. J. Shaw, and D. Ianuzzi, *Phys. Rev. Lett.* **104**, 241101 (2010).
14. Yu. N. Pokotilovski, *Jad. Fiz.* **69**, 953 (2006).
15. V. V. Nesvizhevski, G. Pignol, and K. V. Protasov, *Phys. Rev. D* **77**, 034020 (2008).
16. P. Brax and G. Pignol, *Phys. Rev. Lett.* **107**, 111301 (2011).
17. M. Ahlers, A. Lindner, A. Ringwald, L. Schrempp, and C. Weniger, *Phys. Rev. D* **77**, 015018 (2008).
18. H. Gies, D. F. Mota, and D. S. Shaw, *Phys. Rev. D* **77**, 025016 (2008).
19. J. H. Steffen, A. Upadhye, A. Baumbaugh, A. S. Chou, P. O. Mazur, R. Tomlin, A. Weltman, and A. Wester, *Phys. Rev. Lett.* **105**, 261803 (2010).
20. A. Upadhye, J. H. Steffen, and A. Chou, arXiv:1204.5476 [hep-ph].
21. G. Rybka, M. Hotz, L. J. Rosenberg, S. J. Asztalos, G. Carosi, C. Hagmann, D. Kinton, K. van Bibber, J. Hoskins, C. Martin, P. Sikivie, D. B. Tanner, R. Bradley, and J. Clarke, *Phys. Rev. Lett.* **105**, 051801 (2010).
22. S. A. Werner, J.-L. Staudenmann, and R. Colella, *Phys. Rev. Lett.* **42**, 1103 (1979); D. K. Atwood, M. A. Horne, C. G. Shull, and J. Arthur, *Phys. Rev. Lett.* **52**, 1673 (1984).

23. A. Steyerl, H. Nagel, F.-X. Schreiber, K.-A. Steinhäuser, R. Gähler, W. Gläser, P. Ageron, J.-M. Astruc, N. Drexel, R. Gervais, and W. Mampe, *Phys. Lett. A* **116**, 347 (1986).
24. J. Leitner and S. Okubo, *Phys. Rev.* **136**, B1542 (1964).
25. D. Chang, R. N. Mohapatra, and S. Nussinov, *Phys. Rev. Lett.* **55**, 2835 (1985).
26. C. T. Hill and G. G. Ross, *Nucl. Phys. B* **311**, 253 (1988).
27. P. Fayet, *Class. Quant. Gravit.* **13**, A19 (1996).
28. B. A. Dobrescu and I. Mocioiu, *J. High Energy Phys.* **11**, 005 (2006).
29. S. Weinberg, *Phys. Rev. Lett.* **40**, 223 (1978); F. Wilczek, *Phys. Rev. Lett.* **40**, 279 (1978).
30. C. Hangmann, H. Murayama, G. G. Raffelt, L. J. Rosenberg, and K. van Bibber (Particle Data Group), *J. Phys. G* **37**, 496 (2010).
31. P. Sikivie, *Phys. Rev. Lett.* **51**, 1415 (1983).
32. M. Pospelov, A. Ritz, and M. Voloshin, *Phys. Rev. D* **78**, 115012 (2008).
33. J. E. Moody and F. Wilczek, *Phys. Rev. D* **30**, 130 (1984).
34. E. G. Adelberger, J. H. Gundlach, B. P. Heckel, S. Hoedl, and S. Schlamminger, *Progr. Part. and Nucl. Phys.* **62**, 102 (2009).
35. E. G. Adelberger, B. P. Heckel, and A. E. Nelson, *Ann. Rev. Nucl. Part. Sci.* **53**, 77 (2003).
36. J. Jaeckel and A. Ringwald, *Ann. Rev. Nucl. Part. Sci.* **60**, 405 (2010).
37. G. Raffelt, *Phys. Rev. D* **86**, 015001 (2012).
38. S. Baeßler, V. V. Nesvizhevsky, K. V. Protasov, and A. Yu. Voronin, *Phys. Rev. D* **75**, 075006 (2007).
39. A. P. Serebrov, *Phys. Lett. B* **680**, 423 (2009).
40. V. K. Ignatovich and Yu. N. Pokotilovski, *Eur. Phys. J. C* **64**, 19 (2009).
41. O. Zimmer, *Phys. Lett. B* **685**, 38 (2010); A. P. Serebrov, O. Zimmer, P. Geltenbort, A. K. Fomin, S. N. Ivanov, E. A. Kolomensky, M. S. Lasakov, V. M. Lobashev, A. N. Pirozhkov, V. E. Varlamov, A. V. Vasiliev, O. M. Zherebtsov, E. B. Aleksandrov, S. P. Dmitriev, and N. A. Dovator, *Pis'ma v Zh. Eksp. Teor. Fiz.* **91**, 8 (2010).
42. Yu. N. Pokotilovski, *Phys. Lett. B* **686**, 114 (2010).
43. C. B. Fu, T. R. Gentile, and W. M. Snow, *Phys. Rev. D* **83**, 031504 (2011).
44. A. K. Petukhov, G. Pignol, D. Jullien, and K. H. Andersen, *Phys. Rev. Lett.* **105**, 170401 (2010); A. K. Petukhov, G. Pignol, and R. Golub, *Phys. Rev. D* **84**, 058501 (2011).
45. G. G. Raffelt, *Phys. Rep.* **333–334**, 593 (2000).
46. K. Akama, arXiv:hep-th/0001113.
47. V. A. Rubakov and M. E. Shaposhnikov, *Phys. Lett. B* **125**, 136 (1983).
48. M. Visser, *Phys. Lett. B* **159**, 22 (1985).
49. I. Antoniadis, S. Dimopoulos, and G. Dvali, *Nucl. Phys. B* **516**, 70 (1998).
50. N. Arkani-Hamed, S. Dimopoulos, and G. Dvali, *Phys. Lett. B* **429**, 263 (1998).
51. I. Antoniadis, N. Arkani-Hamed, S. Dimopoulos, and G. Dvali, *Phys. Lett. B* **436**, 257 (1998).
52. N. Arkani-Hamed, S. Dimopoulos, and G. Dvali, *Phys. Rev. D* **59**, 086004 (1999).
53. L. Randall and R. Sundrum, *Phys. Rev. Lett.* **83**, 3370, 4690 (1999).
54. D. J. Kapner, T. S. Cook, E. G. Adelberger, J. H. Gundlach, B. R. Heckel, C. D. Hoyle, and H. E. Swanson, *Phys. Rev. Lett.* **98**, 021101 (2007).
55. V. V. Nesvizhevsky, *Rev. Mod. Phys. A* **27**, 1230006 (2012).
56. J. Jacubek, P. Schmidt-Wellenburg, P. Geltenbort, M. Platkevic, C. Plonka-Spehr, J. Solc, and T. Soldner, *Nucl. Instr. Meth. A* **600**, 651 (2009); T. Sanuki, S. Kamamiya, S. Kawasaki, and S. Sonoda, *Nucl. Instr. Meth. A* **600**, 657 (2009); J. Jacubek, M. Platkevic, P. Schmidt-Wellenburg, P. Geltenbort, C. Plonka-Spehr, and M. Daum, *Nucl. Instr. Meth. A* **607**, 45 (2009); S. Kawasaki, G. Ichikawa, M. Hino, Y. Kamiya, M. Kitaguchi, S. Kawamiya, T. Sanuki, and S. Sonoda, *Nucl. Instr. Meth. A* **615**, 42 (2010).
57. V. V. Nesvizhevsky, A. K. Petukhov, H. G. Börner, T. A. Baranova, A. M. Gagarski, G. A. Petrov, K. V. Protasov, A. Yu. Voronin, S. Baeßler, H. Abele, A. Westphal, and L. Lucovac, *Eur. Phys. J. C* **40**, 479 (2005).
58. W. Drexel, *Neutron News* **1**, 1 (1990).
59. U. Bonse and M. Hart, *Appl. Phys. Lett.* **6**, 155 (1965).
60. H. Rauch, W. Treimer, and U. Bonse, *Phys. Lett. A* **47**, 369 (1974).

61. A. I. Ioffe, Nucl. Instr. Meth. A **268**, 169 (1988).
62. K. Eder, M. Gruber, A. Zeilinger, P. Geltenbort, R. Gähler, W. Mampe, and W. Drexel, Nucl. Instr. Meth. A **284**, 171 (1989).
63. G. van der Zouw, M. Weber, J. Felber, R. Gähler, P. Geltenbort, and A. Zeilinger, Nucl. Instr. Meth. A **440**, 568 (2000).
64. E. H. Cook-Yahrborough, in *Instrumentation Techniques in Nuclear Pulse Analysis*, Washington (1964), p. 207.
65. A. I. Mogilner, O. A. Sal'nikov, and L. A. Timokhin, Pribory i Tekhnika Eksp. No. 2, 22 (1966).
66. M. I. Novopoltsev and Yu. N. Pokotilovski, Pribory i Tekhnika Eksp. No. 5, 19 (2010).
67. M. Pietroni, Phys. Rev. D **72**, 043535 (2005).
68. K. A. Olive and M. Pospelov, Phys. Rev. D **77**, 043534 (2008).
69. K. Hinterbichler and J. Khoury, Phys. Rev. Lett. **104**, 231301 (2010).
70. A. Upadhye, arXiv: 1210.7804 [hep-ph].
71. A. I. Vainshtein, Phys. Lett. B **39**, 393 (1972).
72. A. Nicolis, R. Rattazzi, and E. Trincherini, Phys. Rev. D **79**, 064036 (2009).
73. C. Deffayet, G. Esposito-Farese, and A. Vikman, Phys. Rev. D **79**, 084003 (2009).
74. N. Chow and J. Khoury, Phys. Rev. D **80**, 024037 (2009).
75. C. Bourrage and D. Seery, J. Cosmol. Astrophys. **08**, 011 (2010).
76. E. Babichev, Phys. Rev. D **83**, 024008 (2011).
77. M. Wyman, Phys. Rev. Lett. **106**, 201102 (2011).
78. P. Brax, C. Bourrage, and A.-C. Davis, J. Cosmol. Astrophys. **09**, 020 (2011).
79. A. Ali, R. Gannouji, Md. W. Hossain, and M. Sami, Phys. Lett. B **718**, 5 (2012).